Dynamic Multi-Objective Optimization of Batch Chromatographic Separation Processes

Holmqvist, Anders; Magnusson, Fredrik; Nilsson, Bernt

Published in:
Computer Aided Chemical Engineering

DOI:
10.1016/B978-0-444-63578-5.50131-6

2015

Document Version:
Peer reviewed version (aka post-print)

Krist V. Gernaey, Jakob K. Huusom and Rafiqul Gani (Eds.), 12th International Symposium on Process Systems Engineering and 25th European Symposium on Computer Aided Process Engineering.
31 May - 4 June 2015, Copenhagen, Denmark.

Dynamic Multi-Objective Optimization of Batch Chromatographic Separation Processes

A. Holmqvist[a,*], F. Magnusson[b] and B. Nilsson[a]

[a]*Department of Chemical Engineering, Lund University, P.O. Box 124, SE-221 00 Lund, Sweden*
[b]*Department of Automatic Control, Lund University, P.O. Box 118, SE-221 00 Lund, Sweden*
Anders.Holmqvist@chemeng.lth.se

Abstract

This contribution presents a novel offline dynamic multi-objective optimization framework for high-pressure liquid chromatographic (HPLC) processes in batch elution mode. The framework allows for optimization of general elution trajectories parametrized with piecewise constant control signals. It is based on a simultaneous method where both the control and state variables are fully discretized in the temporal domain, using orthogonal collocations on finite elements, and the state variables are discretized in the spatial domain, using a finite volume weighted essentially non-oscillatory (WENO) scheme. The resulting finite dimensional nonlinear program (NLP) is solved using a primal-dual interior point method and automatic differentiation techniques. The advantages of this open-loop optimal control methodology are highlighted through the solution of a challenging ternary complex mixture separation problem for a hydrophobic interaction chromatography (HIC) system. For a bi-objective optimization of the target component productivity and yield, subject to a purity constraint, the set of Pareto solutions generated with general elution trajectories showed considerable improvement in the productivity objective when compared to the Pareto set obtained using conventional linear elution trajectories.

Keywords: Batch chromatography, Dynamic multi-objective optimization, Collocation

1. Introduction

Isolation of a high purity target component from a multicomponent mixture is of significant importance in the pharmaceutical and biochemical industries. Reproducible selectivity in chromatographic separation of closely related product impurities requires optimized elution mode and fractionation or cut-times (Sreedhar et al., 2013). The current state-of-the-art methodology for optimization of HPLC separation has been limited to linear, concave/convex and step elution trajectories (Damtew et al., 2009). The main purpose of the present study is to demonstrate a novel methodology for simultaneous optimization of general elution trajectories, target component pooling decisions, column loading, and batch cycle time. The realistic multi-component system dynamics required for analysis were generated by numerical solution of the *reaction–dispersive model* (Schmidt-Traub et al., 2012). This model is governed by a set of mass-balance partial differential equations (PDEs), with a modified Langmuir isotherm and experimentally validated kinetics. Hence, the proposed methodology implies formulating and solving a large-scale dynamic optimization problem (DOP) constrained by PDEs (Biegler, 2010). However, in chromatographic separation processes, there are several incommensurable objectives which require a trade-off to ensure a satisfactory design. For the purpose of this study, a set of Pareto solutions were generated for bi-objective scenarios, with target component productivity and yield, by means of a weighted sum (WS) scalarization method.

2. Modeling of HPLC Processes

The governing one-dimensional equations in the *reaction–dispersive model* (Schmidt-Traub et al., 2012) of the mobile and stationary phase, derived under the assumptions of infinitely fast diffusion into the particles and rate-limiting adsorption kinetics, defined in the spatial, $z \in [z_0, z_f]$, and temporal, $t \in [t_0, t_f]$, domains are:

$$\frac{\partial c_\alpha}{\partial t} = -\frac{\partial}{\partial z}\left(c_\alpha v_{\text{int}} - \mathscr{D}_{\text{app},\alpha}\frac{\partial c_\alpha}{\partial z}\right) - \frac{(1-\varepsilon_c)}{\varepsilon_c + (1-\varepsilon_c)\varepsilon_p}\frac{\partial q_\alpha}{\partial t}, \tag{1}$$

$$\frac{\partial q_\alpha}{\partial t} = k_{\text{kin},\alpha}\left(H_{0,\alpha}c_\alpha e^{c_S\gamma_\alpha}\left[1+2K_{\text{eq},\alpha}c_\alpha e^{c_S\gamma_\alpha}\right]\left[1-\sum_{\beta\in\{A,B,C\}}\frac{q_\beta}{q_{\max,\beta}}\right]^{\nu_\alpha} - q_\alpha\right), \tag{2}$$

where c_α and q_α are the mobile and stationary phase concentration of component $\alpha \in \{A,B,C,S\}$, v_{int} denotes the interstitial velocity of the fluid, $\mathscr{D}_{\text{app},\alpha}$ the apparent dispersion coefficient, and ε_c and ε_p the column and particle void fractions. The hydrophobic interaction isotherm described in Eq. (2) is based on the Langmuir mobile phase modulator (Melander et al., 1989). Here, c_S denotes the concentration of the non-absorbing modifier (i.e. $\partial q_S/\partial t := 0$), $k_{\text{kin},\alpha}$ the kinetic rate constant, $H_{0,\alpha}$ the Henry's constant, γ_α the solvophobicity parameter, ν_α the binding charge ratio, $q_{\max,\alpha}$ the maximum concentration of adsorbed components, and $K_{\text{eq},\alpha}$ the equilibrium constant. Eq. (1) is complemented with Danckwerts boundary conditions:

$$c_\alpha(t,z_0)v_{\text{int}} - \mathscr{D}_{\text{app},\alpha}\frac{\partial c_\alpha}{\partial z}(t,z_0) = \begin{cases} c_{\text{load},\alpha}v_{\text{int}}\Pi(t,t_0,\Delta t_{\text{load}}) & \text{if } \alpha \in \{A,B,C\}, \\ c_{\text{mix},S}v_{\text{int}} & \text{if } \alpha = S, \end{cases} \tag{3}$$

$$\frac{\partial c_\alpha}{\partial z}(t,z_f) = 0, \tag{4}$$

where $c_{\text{load},\alpha}$ is the injected load concentration and $\Pi(t,t_0,\Delta t_{\text{load}}) \in [0,1]$ a smooth rectangular function in the temporal horizon $[t_0, \Delta t_{\text{load}}]$. The dynamics of the modifier concentration in the upstream mixing tank, $c_{\text{mix},S}$, is governed by:

$$\frac{\mathrm{d}c_{\text{mix},S}}{\mathrm{d}t} = \frac{1}{\tau_{\text{mix}}}\left(u(t) - c_{\text{mix},S}\right), \tag{5}$$

where u is the elution trajectory and τ_{mix} the residence time. Finally, the PDE system was approximated using the method-of-lines and an adaptive, high-order finite volume WENO scheme (Shu, 1998) on a uniform mesh where $z_j = j\Delta z$ is the discretized spatial coordinate and $j \in [1..N_j]$.

3. Dynamic Multi-Objective Optimization

The elution trajectories at the column outlet, $c_\alpha(t,z_f)$ and $\alpha \in \{A,B,C\}$, form the basis for evaluating the incommensurable objective functions of yield, Y_α, and productivity, P_α, with the intermediately eluting component B as target. The objective functions of the αth component collected in the pooling horizon $[t_c, t_f]$ are defined as:

$$\delta_{\text{load},\alpha}\frac{\mathrm{d}Y_\alpha}{\mathrm{d}t} = c_\alpha(t,z_f)v_{\text{int}}A_c\Pi(t,t_c,t_f), \tag{6}$$

$$\frac{\mathrm{d}P_\alpha}{\mathrm{d}t} = \frac{1}{V_c}\frac{1}{(t_f+t_r)}\delta_{\text{load},\alpha}\frac{\mathrm{d}Y_\alpha}{\mathrm{d}t}, \tag{7}$$

where $\delta_{\text{load},\alpha} = c_{\text{load},\alpha}v_{\text{int}}A_c\Delta t_{\text{load}}$ is the total injected sample amount, A_c and V_c the column cross-sectional area and volume, and $t_r = 2z_f v_{\text{int}}^{-1}$ the assigned regeneration and re-equilibration time (Schmidt-Traub et al., 2012) in column volumes (CV). Hence, the aim is to derive an optimal

elution trajectory, u, load duration, Δt_{load}, and pooling horizon, $[t_c, t_f]$ that maximize $Y_\alpha(t_f)$ and $P_\alpha(t_f)$ while fulfilling the constraint imposed on purity of the target component fractionization:

$$X_\alpha(t_f) = \delta_{\text{load},\alpha} Y_\alpha(t_f) \left(\sum_{\beta \in \{A,B,C\}} \delta_{\text{load},\beta} Y_\beta(t_f) \right)^{-1}, \tag{8}$$

where the numerator of the right hand side represents the captured amount of the target component in $[t_c, t_f]$ and the denominator represents the total amount captured. Hence, $X_\alpha(t_f)$ is incorporated in the DOP as a terminal inequality constraint, $X_{L,\alpha} - X_\alpha(t_f) \leq 0$, with an assigned lower purity requirement $X_{L,\alpha}$.

3.1. Dynamic Multi-Objective Optimization Problem Formulation

The WS scalarization method was used to combine the objectives in Eqs. (6 and 7) into a single performance index with a weight $\omega \in [0,1]$ and the resulting optimization problem can be cast in the frame for *min–min optimal control*:

$$\text{min.} \quad -\left(\omega \int_{t_0}^{t_f} \frac{\mathrm{d}P_B}{\mathrm{d}t} \mathrm{d}t + (1-\omega) \int_{t_0}^{t_f} \frac{\mathrm{d}Y_B}{\mathrm{d}t} \mathrm{d}t \right) + \mathcal{U} \sum_{i=2}^{N_u} \Delta u_i^2, \tag{9a}$$

$$\text{w.r.t.} \quad \left(\Delta t_{\text{load}}, t_f\right) \in \mathbb{R}^2,$$

$$\text{s.t.} \quad \Delta t_{\text{load},L} \leq \Delta t_{\text{load}} \leq \Delta t_{\text{load},U}, \quad t_{f,L} \leq t_f \leq t_{f,U}, \tag{9b}$$

$$(\boldsymbol{x}, u, t_c) = \arg\min. \quad -\left(\omega \int_{t_0}^{t_f} \frac{\mathrm{d}P_B}{\mathrm{d}t} \mathrm{d}t + (1-\omega) \int_{t_0}^{t_f} \frac{\mathrm{d}Y_B}{\mathrm{d}t} \mathrm{d}t \right) + \mathcal{U} \sum_{i=2}^{N_u} \Delta u_i^2, \tag{9c}$$

$$\text{w.r.t.} \quad \boldsymbol{x} : [t_0, t_f] \to \mathbb{R}^{n_x},$$

$$t_c \in \mathbb{R}, \qquad u \in \mathbb{R}^{N_u},$$

$$\text{s.t.} \quad \boldsymbol{F}\left(t, \dot{\boldsymbol{x}}(t), \boldsymbol{x}(t), u(t), \Delta t_{\text{load}}, t_f, t_c\right) = \boldsymbol{0}, \quad \boldsymbol{x}(t_0) = \boldsymbol{x}_0, \tag{9d}$$

$$X_{B,L} - X_B(t_f) \leq 0, \tag{9e}$$

$$\boldsymbol{x}_L \leq \boldsymbol{x}(t), \qquad t_{c,L} \leq t_c \leq t_{c,U}, \tag{9f}$$

$$u_L \leq u \leq u_U, \qquad |\Delta u| \leq \Delta u_U, \tag{9g}$$

$$\forall t \in [t_0, t_f], \forall i \in [1..N_i], \qquad \forall z \in [z_0, z_f], \forall j \in [1..N_j].$$

Eqs. (9a and 9c) have a typical optimal control Lagrange term together with a quadratic penalty on the differences of the piecewise constant controls, Δu, in the temporal domain, which is discretized with N_i finite elements. This will influence the smoothness of u, and $\mathcal{U}$ is a weight. The optimization variables are the free operating parameters—the discrete control signal u and free time-invariant parameters $(\Delta t_{\text{load}}, t_f, t_c)$—and the state variables $\boldsymbol{x}(t) = (c_\alpha(t,z_j), c_S(t,z_j), c_{\text{mix},S}(t), q_\alpha(t,z_j), P_B(t), Y_\alpha(t), X_B(t))$ where $\alpha \in \{A,B,C\}$. The trajectories $\boldsymbol{x}$ are determined by the free operating parameters via the implicit differential algebraic equations (DAE) system of index one in Eq. (9d). Time-invariant bounds on variables are introduced in Eq. (9f) and bounds on u and Δu are introduced in Eq. (9g).

In this study, a decomposition strategy is adopted to transform the DOP into two levels: (i) the upper-level static optimization problem (Eqs. (9a–9b)) with respect to $(\Delta t_{\text{load}}, t_f)$ which is solved using a Nelder–Mead Simplex algorithm, and (ii) the lower-level DOP (Eqs. (9c–9g) constrained by the DAE system dynamics is transcribed into a NLP using direct collocation, as described in Section 4, and solved using IPOPT (Wächter and Biegler, 2006). By these means, the lower-level DOP is solved for a fixed temporal horizon $[t_0, t_f]$ which considerably reduces the NLP complexity and hence leads to an efficient computation.

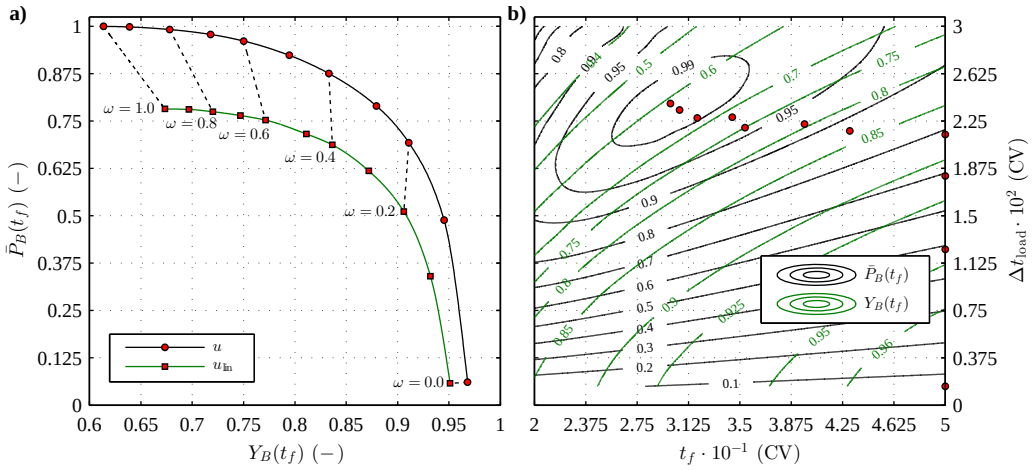

Figure 1: a) Pareto optimal solutions for $\omega \in [0.0, 1.0]$ and $X_{L,B}(t_f) = 9.9 \cdot 10^{-1}$. b) Interpolated sampled contours of $Y_B(t_f)$ and normalized $\bar{P}_B(t_f)$ generated for u as a function of $\Delta t_{\mathrm{load}} \in [0.15, 3.0] \cdot 10^{-2}$ (CV) and $t_f \in [2.0, 5.0] \cdot 10^{1}$ (CV). Markers indicate the Pareto optimal time-invariant optimization variables of the upper-level static optimization problem (Eq. (9a–9b)).

4. Modeling and Optimization Environment

Modelica (The Modelica Association, 2012) was used as the description language for the HPLC process model presented in Section 2. The open-source platform JModelica.org (Åkesson et al., 2010) was used for simulation and optimization of the Modelica model. In the context of simulation, JModelica.org was used to compile the Modelica model into a functional mock-up unit (FMU) (Blochwitz et al., 2011), thus transforming it from a DAE form into an ordinary differential equation (ODE) form. JModelica.org's interface to SUNDIALS (Hindmarsh et al., 2005) was subsequently used to simulate the model.

The formulation of the DOP (Eq. (9c–9g) was made using the Modelica extension Optimica (Åkesson et al., 2010). The algorithm used in the work described in this paper to solve the DOP uses a direct and local collocation method (Biegler, 2010) on finite elements, using Radau points and Lagrange interpolation polynomials (Magnusson and Åkesson, 2012). The algorithm has been implemented in Python in the JModelica.org framework, using the computer algebra system with automatic differentiation (CasADi) optimization package (Andersson et al., 2012). By using CasADi's symbolic syntax, the DOP was transcribed into a finite dimensional NLP. The NLP was subsequently solved using the primal-dual interior point method IPOPT v.3.11.8 (Wächter and Biegler, 2006) and the linear solver MA57 from HSL (HSL, 2013).

5. Results and Discussion

The temporal horizon was discretized with $N_i = 1 \cdot 10^2$ finite elements with two Radau collocations points in each element and a piecewise constant control discretization with $N_u = 5 \cdot 10^1$ pieces was adopted. The spatial domain was discretized with $N_j = 2 \cdot 10^1$ finite volume elements with a 4th order WENO scheme and the resulting NLP has approximately $1 \cdot 10^5$ variables. In order to assess the performance of the general elution trajectories, these were benchmarked with conventional linear trajectories governed by:

$$u_{\mathrm{lin}}(t) = u_{\mathrm{lin}}(t_{\mathrm{lin},0}) + \left[u_{\mathrm{lin}}(t_f) - u_{\mathrm{lin}}(t_{\mathrm{lin},0})\right] \left(\frac{t - t_{\mathrm{lin},0}}{t_f}\right), \tag{10}$$

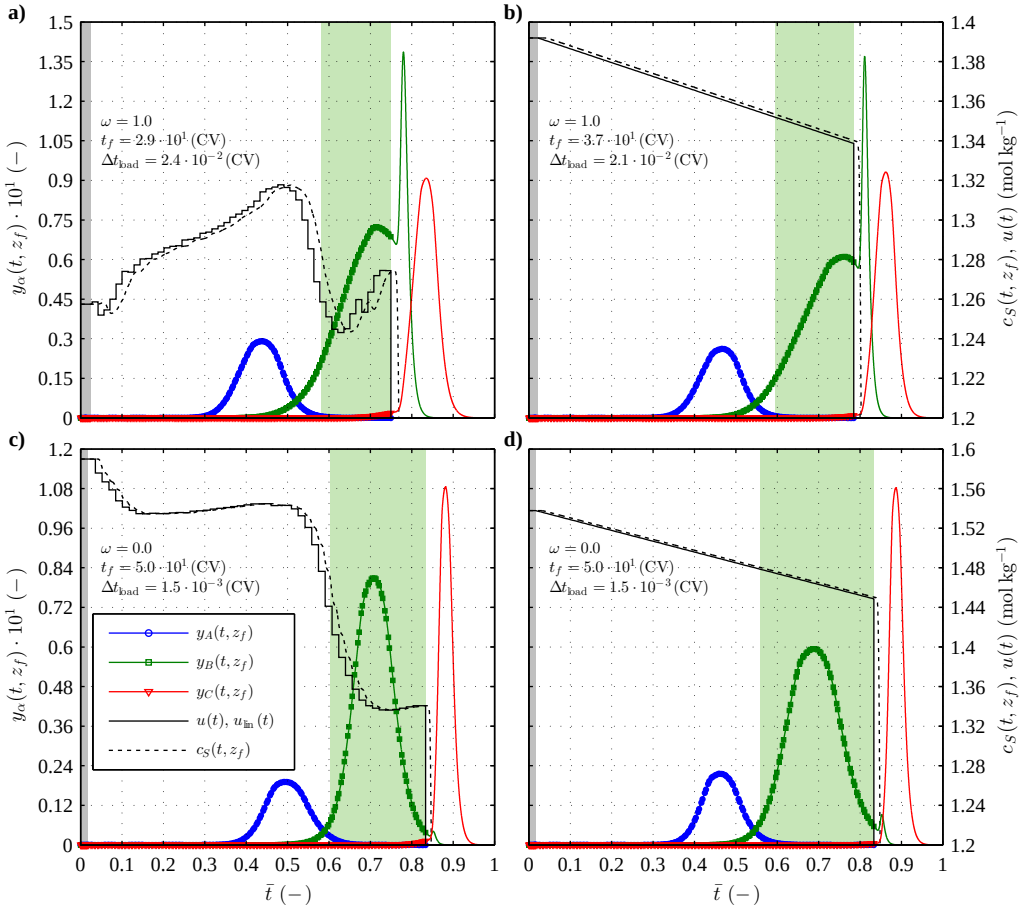

Figure 2: Optimal elution trajectories, where $y_\alpha(t,z_f) = c_\alpha(t,z_f)v_{\text{int}}(A_c^{-1}\sum_{\beta\in\{A,B,C\}}\delta_{\text{load},\beta})^{-1}$ is the normalized flux at $z = z_f$, as a function of normalized time $\bar{t} = t(t_f + t_r)^{-1}$. Markers indicate the solution at the Radau collocation points and solid and dashed lines the simulated response. The shaded areas indicate the pooling interval endpoints, $[t_c, t_f]$, and those of the initial load and wash, $[t_0, t_0 + \Delta t_{\text{load}} + \Delta t_{\text{wash}}]$.

where $t_{\text{lin},0} = t_0 + \Delta t_{\text{load}} + \Delta t_{\text{wash}}$ defines the onset of the elution mode and $(u_{\text{lin}}(t_{\text{lin},0}), u_{\text{lin}}(t_f))$ are the optimization variables. It is evident from analyzing the Pareto optimal fronts for $X_{L,B}(t_f) = 9.9 \cdot 10^{-1}$ depicted in Fig. 1a that the general elution trajectories, u, outperform the linear trajectories, u_{lin}, in terms of both objectives. Especially, for $\omega = 1.0$ the maximum productivity obtained with u is approximately 28% higher than that for u_{lin}. In addition, the dependency of $P_B(t_f)$ and $Y_B(t_f)$ on the time-invariant optimization variables $(\Delta t_{\text{load}}, t_f)$ associated with u depicted in Fig. 1b shows that $Y_B(t_f)$ is strictly decreasing as $\Delta t_{\text{load}} \to \Delta t_{\text{load},U}$ and $t_f \to t_{f,L}$ whereas $P_B(t_f)$ exhibits a convex behavior. The contours in Fig. 1b were generated by interpolating the solution to the lower-level DOP (Eq. (9c–9g) on a dense rectangular grid of $(\Delta t_{\text{load}}, t_f)$.

The associated elution profiles for $\omega = (0.0, 1.0)$ illustrated in Fig. 2 show a clear distinction in the system response generated with u and u_{lin}, respectively. As governed by Eq. (10), u_{lin} and hence the optimal modifier concentration is strictly decreasing in $[t_{\text{lin},0}, t_f]$ in order to increase hydrophobicity and to elute the components $\alpha \in \{A, B, C\}$. Contrarily, the modifier concentration

is freely controlled with the parametrized elution trajectories which ultimately promotes $P_B(t_f)$ through increasing Δt_{load} and reducing t_f while fulfilling the purity constraint (Figs. 2a and 2b). However, maximizing $Y_B(t_f)$ (which is time-invariant) implies injecting a minimal column load, and hence, $(\Delta t_{\text{load}}, t_f)$ are constrained by their lower and upper boundaries, and the gain in $Y_B(t_f)$ for u is therefore only moderate (Figs. 2c and 2d). Finally, it is noteworthy that the DOP (Eq. (9c–9g)) is solved for the temporal horizon $[t_0, t_f]$, and the control signal is prescribed a constant value of $5.0 \cdot 10^{-1}$ $(\text{mol}\,\text{kg}^{-1})$ for $t > t_f$, i.e. the column regeneration and re-equilibration.

6. Concluding Remarks

A novel methodology for rendering large-scale offline dynamic multi-objective optimization problems for HPLC processes in batch elution mode was developed in this paper. The assessment of the set of Pareto solutions generated with general elution trajectories, parametrized with a piecewise constant control signal, showed considerable improvement in the productivity objective when benchmarked with the Pareto set obtained using conventional linear elution trajectories.

Acknowledgement

The authors acknowledge the support of the strategic innovation program Process Industrial IT and Automation (SIO–PiiA) and the LCCC Linnaeus Center and the eLLIIT Excellence Center at Lund University.

References

Åkesson, J., Årzén, K.-E., Gäfvert, M., Bergdahl, T., Tummescheit, H., 2010. Modeling and optimization with Optimica and JModelica.org—Languages and tools for solving large-scale dynamic optimization problems. Computers & Chemical Engineering 34 (11), 1737–1749.

Andersson, J., Åkesson, J., Diehl, M., 2012. CasADi: A Symbolic Package for Automatic Differentiation and Optimal Control. In: Forth, S., Hovland, P., Phipps, E., Utke, J., Walther, A. (Eds.), Recent Advances in Algorithmic Differentiation. Vol. 87 of Lecture Notes in Computational Science and Engineering. Springer Berlin Heidelberg, pp. 297–307.

Biegler, L. T., 2010. Nonlinear Programming: Concepts, Algorithms, and Applications to Chemical Processes. MOS-SIAM Series on Optimization, Mathematical Optimization Society and the Society for Industrial and Applied Mathematics, PA, USA.

Blochwitz, T., Otter, M., Arnold, M., Bausch, C., Clau, C., Elmqvist, H., Junghanns, A., Mauss, J., Monteiro, M., Neidhold, T., Neumerkel, D., Olsson, H., Peetz, J.-V., Wolf, S., March 2011. The Functional Mockup Interface for tool independent exchange of simulation models. In: Proceedings of the 8th International Modelica Conference. Dresden, Germany.

Damtew, A., Sreedhar, B., Seidel-Morgenstern, A., 2009. Evaluation of the potential of nonlinear gradients for separating a ternary mixture. Journal of Chromatography A 1216 (28), 5355–5364.

Hindmarsh, A. C., Brown, P. N., Grant, K. E., Lee, S. L., Serban, R., Shumaker, D. E., et al., 2005. SUNDIALS: Suite of nonlinear and differential/algebraic equation solvers. ACM Transactions on Mathematical Software 31 (3), 363–396.

HSL, 2013. A collection of fortran codes for large scale scientific computation. URL: `http://www.hsl.rl.ac.uk`.

Magnusson, F., Åkesson, J., Sep 2012. Collocation methods for optimization in a Modelica environment. In: 9th International Modelica Conference. Munich, Germany.

Melander, W. R., El Rassi, Z., Horváth, C., 1989. Interplay of hydrophobic and electrostatic interactions in biopolymer chromatography: Effect of salts on the retention of proteins. Journal of Chromatography A 469, 3–27.

Schmidt-Traub, H., Schulte, M., Seidel-Morgenstern, A., 2012. Preparative Chromatography, 2nd Edition. Wiley-VCH, Weinheim.

Shu, C.-W., 1998. Essentially non-oscillatory and weighted essentially non-oscillatory schemes for hyperbolic conservation laws. In: Quarteroni, A. (Ed.), Advanced Numerical Approximation of Nonlinear Hyperbolic Equations. Vol. 1697 of Lecture Notes in Mathematics. Springer Berlin Heidelberg, pp. 325–432.

Sreedhar, B., Wagler, A., Kaspereit, M., Seidel-Morgenstern, A., 2013. Optimal cut-times finding strategies for collecting a target component from overloaded elution chromatograms. Computers & Chemical Engineering 49, 158–169.

The Modelica Association, 2012. The Modelica Association Home Page. URL: `http://www.modelica.org`.

Wächter, A., Biegler, L. T., 2006. On the implementation of an interior-point filter line-search algorithm for large-scale nonlinear programming. Mathematical Programming 106 (1), 25–57.